Acta Crystallographica Section F
Structural Biology and Crystallization Communications
ISSN 1744-3091

Cloning, purification, crystallization and preliminary crystallographic analysis of the human histone deacetylase sirtuin 1

Kenneth P. Holbourn,[a] Matthew D. Lloyd,[b] Andrew S. Thompson,[b] Michael D. Threadgill[b] and K. Ravi Acharya[a]*

[a]Department of Biology and Biochemistry, University of Bath, Bath BA2 7AY, England, and [b]Medicinal Chemistry, Department of Pharmacy and Pharmacology, University of Bath, Bath BA2 7AY, England

Correspondence e-mail: bsskra@bath.ac.uk

Received 13 December 2010
Accepted 25 January 2011

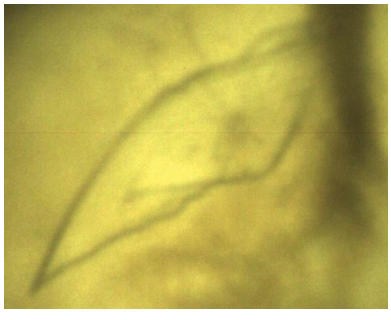

Human sirtuin 1 is a member of the histone deacetylase family and is involved in cellular aging, tumourigenesis and cellular metabolism. Recombinant sirtuin 1 comprising residues 140–747 was crystallized using the hanging-drop vapour-diffusion method. The crystal diffracted to 3.4 Å resolution and belonged to space group *P*622, with unit-cell parameters $a = b = 203.1$, $c = 625.3$ Å, and is estimated to contain between six and 12 molecules per asymmetric unit.

1. Introduction

Sirtuin 1 is the most extensively studied member of the class III histone deacetylase (HDAC) family. The sirtuins or Sir2 enzymes are a specialized class of NAD^+-dependent deacetylases that specifically act on acetyl-lysine residues (Frye, 1999). They catalyse the hydrolysis of NAD^+ and the transfer of an acetyl group from the substrate to the ADP-ribose fragment (Sauve *et al.*, 2001). In addition, many of the sirtuins also possess ADP-ribosyl transferase activity: that is, they are able to transfer the ADP-ribose moiety onto a substrate protein (Tanny *et al.*, 1999).

Sirtuins are highly conserved and have been identified in both eukaryotes and prokaryotes (Dutnall & Pillus, 2001). Although the sirtuins were originally classified as HDACs, their substrates now include a diverse range of proteins that are responsible for many different cellular functions including gene silencing, cell-cycle regulation, cell metabolism, apoptosis, tumourigenesis and regulation of lifespan (Taylor *et al.*, 2008). This has led to the sirtuins being studied as potential therapeutic targets in neurodegenerative disease, inflammation, type 2 diabetes and some cancers. There are seven sirtuins found in human cells. They are distinct from one another in both cellular location and function. Sirtuins 1, 6 and 7 are present in the nucleus, sirtuin 2 in the cytoplasm and sirtuins 3, 4 and 5 in mitochondria (Taylor *et al.*, 2008). Sirtuin 1 is the most well studied human sirtuin, with the focus being on its role in cellular aging and cancer.

To date, several sirtuin structures have been determined, including those of human sirtuins 2 (Finnin *et al.*, 2001), 3 (Jin *et al.*, 2009) and 5 (Schuetz *et al.*, 2007). These all share an ∼250-residue catalytic core that is comprised of two domains. The larger domain contains an NAD^+-binding 'Rossmann fold', whilst the smaller domain contains a zinc-binding site. The active site where the protein substrate binds lies in a cleft between the two domains. While sirtuin 1 possesses this central catalytic core (residues 244–295), it is much larger than the other human sirtuins at 747 residues in length, with extensive N- and C-terminal domains (Autiero *et al.*, 2009). There are currently no structural data for sirtuin 1, although protein modelling and data mining have suggested that the N- and C-terminal regions are largely unstructured (Autiero *et al.*, 2009). However, they contain a key allosteric binding site and other sites where activators and regulators interact, including the well known drug resveratrol. Resveratrol has been shown to extend cellular lifespan in yeast and *Caenorhabditis elegans* and has been suggested to have neuroprotective and anti-cancer properties (Howitz *et al.*, 2003).

In order to elucidate the structure of the human sirtuin 1 molecule and to determine whether there are any underlying structures or new folds present in the N- and C-terminal regions, the sirtuin 1 gene (residues 140–747) has been cloned and the protein has been expressed, purified and crystallized.

2. Materials and methods

All chemicals and reagents were obtained from the Sigma–Aldrich Chemical Company and were used without further purification, unless otherwise noted. Media and other sterile reagents were autoclaved at 394 K for 20 min; solutions of antibiotics and other temperature-sensitive reagents were sterilized using a 0.22 µm filter when required.

2.1. Cloning

A cDNA clone comprising residues 140–747 was obtained from Autogen Bioclear and was used for polymerase chain reaction (PCR) amplification using the oligonucleotide primers 5′-GACGACGACAAGATGATTGGGTACCGAGATAACCTTCTG (forward) and 5′-GAGGAGAAGCCCGGTCTATGATTTGTTTGATGGATAGTTCATGTCTGTTACTTCC (reverse) with KOD polymerase (Merck Biosciences) in the presence of 1 *M* betaine. The amplified product was treated with *Dpn*I enzyme for 90 min at 310 K before being cloned into the pTriEx-4 EK/LIC vector (Merck Biosciences). The resulting plasmid was analysed by DNA sequencing to confirm the insertion of the Sirt1 gene (MWG). This rSirt1 comprised residues 140–747 with the addition of an N-terminal His_6 tag and a short eight-residue linker sequence.

2.2. Expression and purification

The rSirt1 plasmid was transformed into *Escherichia coli* RosettaGami cells (Merck Biosciences). A single colony was used to inoculate 10 ml LB medium supplemented with 100 µg ml^{-1} ampicillin and grown overnight. The overnight culture was then used to inoculate 1 l ZYM-5052 autoinduction medium (Studier, 2005). The culture was grown at 310 K for ∼10 h before being grown for a further ∼16 h at 301 K. Cells were harvested by centrifugation and pellets were stored at 253 K until needed. Cell pellets were defrosted and resuspended in 40 ml lysis buffer (20 m*M* Tris–HCl, 500 m*M* NaCl, 20 m*M* imidazole–HCl pH 8.0 supplemented with 0.3 mg ml^{-1} lysozyme and 20 U DNAse) and stirred at room temperature for ∼20 min before being passed twice through a French Press at ∼17 MPa followed by centrifugation. The supernatant was loaded onto an ÄKTAxpress (GE Healthcare) for a two-stage protein-purification protocol. This comprised Ni^{2+}-affinity chromatography using a 1 ml HiTrap crude column (GE Healthcare) pre-equilibrated with lysis buffer and eluted with a 20–500 m*M* imidazole gradient in a buffer consisting of 50 m*M* Tris–HCl and 200 m*M* NaCl pH 8.0. Peak fractions were then automatically pooled and applied onto a Superdex 75 gel-filtration column that had been equilibrated with 50 m*M* Tris–HCl, 200 m*M* NaCl pH 8.0. All purification steps were performed at 291 K. Fractions containing pure rSirt1 were pooled and the protein was further concentrated to 3 mg ml^{-1}. Purity was assessed using an SDS–PAGE gel, anti-His Western blotting and anti-Sirt1 antibody blotting.

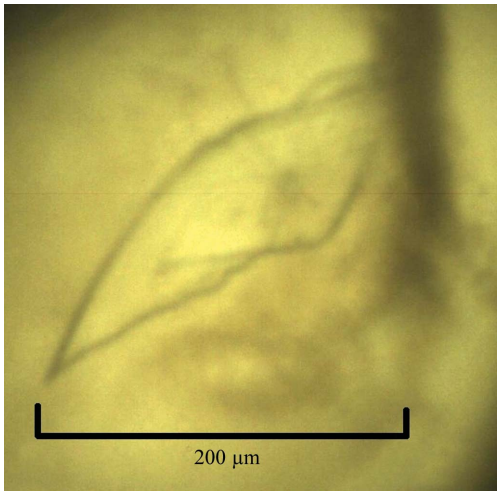

Figure 1
Crystal of rSirt1.

Table 1
Crystal parameters and data-collection statistics for the crystal of rSirt1.

Values in parentheses are for the highest resolution shell.

Space group	*P*622
Unit-cell parameters (Å, °)	a = 203.1, b = 203.1, c = 625.3, $\alpha = \beta = 90$, $\gamma = 120$
Resolution (Å)	3.45 (3.64–3.45)
Total reflections	272760
Unique reflections	79215
Multiplicity	3.4 (1.6)
Average $I/\sigma(I)$	6.3 (2.3)
Average mosaicity (°)	0.37
Completeness (%)	79.4 (58.7)
R_{merge}† (%)	14.6 (24.5)
$R_{p.i.m.}$ (%)	7.5 (20.5)
R_{meas} (%)	16.6 (32.1)
Wilson B factor (Å^2)	50.9

† $R_{merge} = \sum_{hkl}\sum_i |I_i(hkl) - \langle I(hkl)\rangle| / \sum_{hkl}\sum_i I_i(hkl)$, where $I_i(hkl)$ and $\langle I(hkl)\rangle$ are the ith and the mean measurements of the intensity of reflection hkl, respectively.

2.3. Crystallization

Crystallization screening experiments were initially carried out *via* the sitting-drop vapour-diffusion method using a Phoenix robot (Art Robbins) with Structure Screen I + II, Morpheus, PGA Screen, PACT premier and JSCG+ (Molecular Dimensions). All crystallization trials were carried out at 289 K. For screening, 150 nl protein solution (3 mg ml^{-1} protein in 50 m*M* Tris–HCl, 200 m*M* NaCl pH 8.0) was mixed with 150 nl well solution and equilibrated against 60 µl reservoir solution. Microcrystals appeared within around one month in well D4 of the Morpheus screen (0.1 *M* buffer 1 pH 6.5, 0.12 *M* alcohols, 37.5% MPD/PEG 1K/PEG 3350). Larger crystals were produced using manually set-up 24-well plates with the hanging-drop vapour-diffusion method. 1.2 µl protein solution supplemented with 20 m*M* NAD^+ was mixed with 1.2 µl Morpheus screen condition D4 and equilibrated against an 800 µl reservoir. A large dagger-shaped crystal (Fig. 1) appeared after around two weeks.

2.4. X-ray data collection and processing

The crystal of rSirt1 was transferred to a cryoprotectant solution [Morpheus screen condition D4 + 20%(*v*/*v*) glycerol] before being used for diffraction data collection at 100 K on beamline I02 at the Diamond Light Source (Didcot, England). A total of 686 images from a single crystal were recorded with an oscillation angle of 0.1° per image, a crystal-to-detector distance of 542 mm and an exposure time of 1 s. The diffraction data were processed with the *MOSFLM* processing package (Leslie, 1992) and then merged in the *CCP*4 program suite using *SCALA* (Collaborative Computational Project,

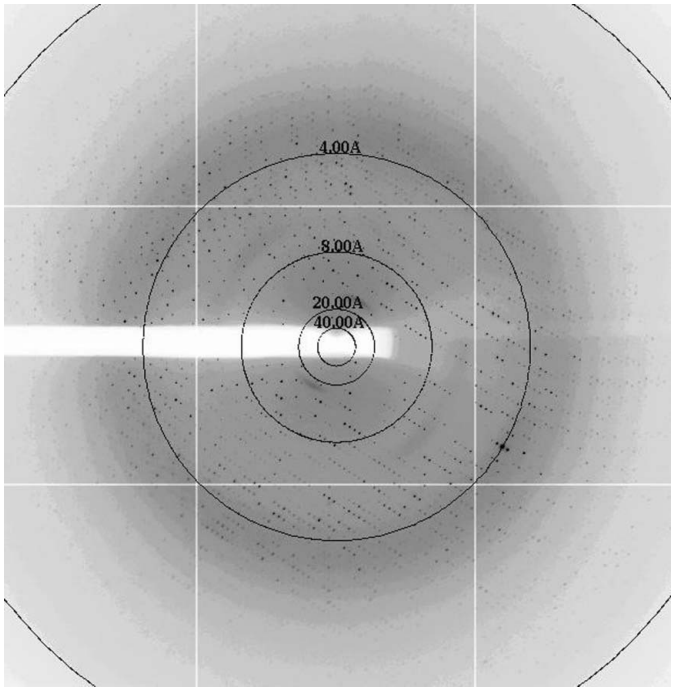

Figure 2
X-ray diffraction image collected from a crystal of rSirt1.

Number 4, 1994). Data-collection and processing statistics are listed in Table 1.

3. Results and discussion

Despite the importance of Sirt1 and the large number of reported functional studies, no structure has been reported. The clone used started at residue 139 and excluded the eukaryotic signal sequence and the poly-Ala, poly-Asp and poly-Glu regions, but included the allosteric binding site. The protein expressed with a low yield and required careful optimization to produce pure rSirt1. Purified protein was concentrated to $\sim$3 mg ml^{-1} for crystallization trials and was characterized by Western blotting using anti-His-tag and anti-Sirt1 antibody staining. The initial automated high-throughput crystal screening gave hits in several conditions. Condition D4 from the Morpheus screen was then used in larger volume crystallization trials. The crystal of rSirt1 grew over the course of around two weeks (Fig. 1) and diffracted to $\sim$3.4 Å resolution (Fig. 2).

Owing to the large unit cell, data processing was unsuccessful in *HKL*-2000 and *d*TREK* but was finally achieved in *MOSFLM* (Leslie, 1992; Table 1). The calculated Matthews coefficient (Matthews, 1968) suggests the presence of between six and 12 protein molecules per asymmetric unit. We are currently attempting to solve the structure of rSirt1 by molecular replacement of the core catalytic domain in combination with other methods of phasing.

This work was supported by Cancer Research UK through a Discovery Committee project grant (C1119/A9872). We thank the scientists at beamline I02 of the Diamond Light Source and Dr Nethaji Thiyagarajan for their help during data collection.

References

Autiero, I., Costantini, S. & Colonna, G. (2009). *PLoS One*, **4**, e7350.
Collaborative Computational Project, Number 4 (1994). *Acta Cryst.* D**50**, 760–763.
Dutnall, R. N. & Pillus, L. (2001). *Cell*, **105**, 161–164.
Finnin, M. S., Donigian, J. R. & Pavletich, N. P. (2001). *Nature Struct. Biol.* **8**, 621–625.
Frye, R. A. (1999). *Biochem. Biophys. Res. Commun.* **260**, 273–279.
Howitz, K. T., Bitterman, K. J., Cohen, H. Y., Lamming, D. W., Lavu, S., Wood, J. G., Zipkin, R. E., Chung, P., Kisielewski, A., Zhang, L.-L., Scherer, B. & Sinclair, D. A. (2003). *Nature (London)*, **425**, 191–196.
Jin, L., Wei, W., Jiang, Y., Peng, H., Cai, J., Mao, C., Dai, H., Choy, W., Bemis, J. E., Jirousek, M. R., Milne, J. C., Westphal, C. H. & Perni, R. B. (2009). *J. Biol. Chem.* **284**, 24394–24405.
Leslie, A. G. W. (1992). *Jnt CCP4–ESF/EACBM Newsl. Protein Crystallogr.* **26**.
Matthews, B. W. (1968). *J. Mol. Biol.* **33**, 491–497.
Sauve, A. A., Celic, I., Avalos, J., Deng, H., Boeke, J. D. & Schramm, V. L. (2001). *Biochemistry*, **40**, 15456–15463.
Schuetz, A., Min, J., Antoshenko, T., Wang, C.-L., Allali-Hassani, A., Dong, A., Loppnau, P., Vedadi, M., Bochkarev, A., Sternglanz, R. & Plotnikov, A. N. (2007). *Structure*, **15**, 377–389.
Studier, F. W. (2005). *Protein Expr. Purif.* **41**, 207–234.
Tanny, J. C., Dowd, G. J., Huang, J., Hilz, H. & Moazed, D. (1999). *Cell*, **99**, 735–745.
Taylor, D. M., Maxwell, M. M., Luthi-Carter, R. & Kazantsev, A. G. (2008). *Cell. Mol. Life Sci.* **65**, 4000–4018.